Advances in Energy and Materials Research
https://jaem.qom.ac.ir/

Numerical Analysis of Coil Conductivity Effects on Energy Efficiency and Thermal Performance in Induction-Based Crystal Growth Systems

Hossein Karbaschi [1] and Mohammad Hossein Tavakoli [2]

1. *Corresponding Author, Faculty of Science, Mahallat Institute of Higher Education, Mahallat, 37811-51958, Iran Email: H.Karbaschi@mahallat.ac.ir*
2. *Physics Department, Bu-Ali Sina University, Hamedan 65174, Iran, Email: mht@basu.ac.ir*

Article Info

Article type:
Research Article

Article history:
Received 25 Jan 2025
Received in revised form 26 Mar 2025
Accepted 1 May 2025
Published online 25 Jun 2025

Keywords:
Induction heating, Czochralski, Crystal Growth, Electrical Conductivity, Induction Coil.

ABSTRACT

Induction heating is a key technology in Czochralski crystal growth systems, in which precise control of the thermal field inside the crucible is essential for achieving high crystal quality. While the influence of parameters such as excitation frequency, coil geometry, and input power has been widely investigated, the effect of the electrical conductivity of the induction coil has received comparatively less attention. In this study, the impact of induction coil electrical conductivity on heat generation, spatial heat distribution, and heating efficiency in an induction-heated Czochralski system is systematically investigated using a coupled electromagnetic numerical model. The governing Maxwell equations are formulated under steady-state and axisymmetric assumptions and solved using the finite element method. The electrical conductivity of the induction coil is varied over several orders of magnitude, while the crucible material properties are kept constant. The results demonstrate that increasing the coil conductivity significantly enhances the total heat generated within the crucible, improves the uniformity of heat distribution, and substantially reduces ohmic losses within the coil. A saturation-like behavior is observed at higher conductivity values, indicating diminishing returns beyond a certain threshold. The heating efficiency of the system increases dramatically from only a few percent at low conductivities to values exceeding 90% at high conductivities. These findings highlight the critical role of induction coil electrical conductivity in optimizing energy efficiency and thermal stability in Czochralski crystal growth systems and provide practical guidelines for the design of high-performance induction heating configurations.

Cite this article: Karbaschi, H., & Tavakoli, M. H. (2025). Numerical Analysis of Coil Conductivity Effects on Energy Efficiency and Thermal Performance in Induction-Based Crystal Growth Systems. Advances in Energy and Materials Research, 2(6)28-35.
https://doi.org/10.22091/jaem.2026.15272.1040

DOI: 10.22091/jaem.2026.15272.1040
Publisher: University of Qom.

1. Introduction

Radio-frequency induction heating is a non-contact heating technique that has been widely employed in various materials-processing applications, including heat treatment, joining, welding, brazing, soldering, melting, and non-destructive testing. Owing to its advantages such as cleanliness, rapid heating rates, high energy efficiency, and precise controllability, induction heating has become an indispensable technology in both industrial and research environments.

A typical induction heating system consists of three main components: an induction coil, an alternating-current (AC) power supply, and a workpiece in which heat is generated. When the coil is connected to the AC source, a time-varying electromagnetic field is established around it. This field penetrates the metallic components of the system and induces eddy currents within them. The interaction between these induced currents and the electrical resistance of the material results in Joule heating, leading to volumetric heat generation with pronounced spatial and temporal variations.

In certain applications, heating is achieved indirectly rather than by direct induction in the target material. In such configurations, heat is first generated in an electrically conductive container or susceptor and then transferred to the material of interest by conduction and radiation. The Czochralski process is one of the most widely used crystal growth techniques for producing high-quality single crystals of semiconductors, metals, salts, and various oxide materials. Owing to its technological importance in semiconductor manufacturing, the Czochralski method has been extensively studied and documented.

Induction heating is commonly employed in Czochralski crystal growth systems because it enables flexible control of the thermal field within the crucible. As schematically illustrated in Figure 1, an electrically conductive crucible serves as the container in these systems. The crystal growth process is highly sensitive to both the magnitude and spatial distribution of the induced heat within the crucible, as these factors strongly influence thermal gradients, melt convection, and the shape of the solid–liquid interface. The induction heating process is governed by a complex coupling between electromagnetic and thermal phenomena, and its performance depends on numerous system and material parameters.

Previous studies have examined the influence of excitation frequency, coil geometry, coil–workpiece distance, and input power on the distribution of induced currents and heat generation [1–6]. Induction heating has also been effectively utilized across a variety of industrial and scientific applications, such as induction brazing [7], surface hardening [8, 9], and induction melting [10, 11]. In the context of crystal growth, several numerical and experimental investigations have focused on optimizing crucible design, susceptor materials, and heating configurations to achieve improved temperature uniformity and enhanced crystal quality [12–19].

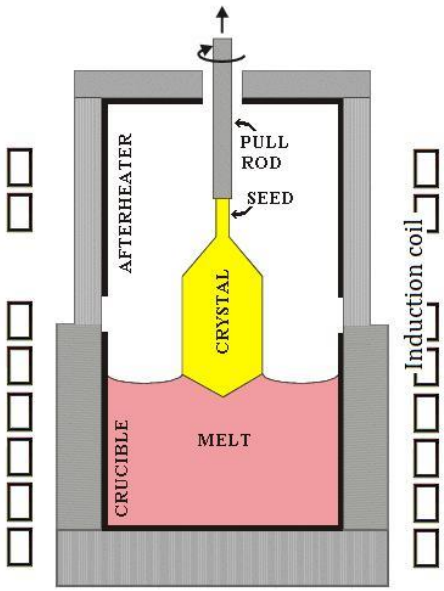

Figure 1: Schematic illustration of a typical induction-heated Czochralski crystal growth system, including the induction coil, crucible, and axisymmetric geometry.

To gain deeper insight into the complex multiphysical nature of induction heating in crystal growth technology and to identify optimal operating conditions, two main approaches are generally adopted: (1) experimental trial-and-error methods and (2) numerical simulation. Although experimental approaches provide valuable practical insights, they are often costly, time-consuming, and limited in their ability to isolate the influence of individual parameters. In contrast, numerical simulation offers a cost-effective and flexible framework for systematically analyzing the induction heating process and accurately capturing the underlying electromagnetic–thermal interactions. Despite extensive research on induction heating parameters, the specific influence of the electrical conductivity of the induction coil has received comparatively limited attention, particularly in the context of Czochralski crystal growth systems. In this study, the effect of induction coil electrical conductivity on induced heat generation within the crucible is systematically investigated. To this end, the governing equations of the induction heating process are first reviewed, and the coupled electromagnetic–thermal problem is subsequently solved using the finite element method.

2. Mathematical methods

The electromagnetic behavior of the induction heating process has been extensively investigated in previous studies [3–6]. In this work, a well-established formulation based on Maxwell's equations is briefly reviewed and subsequently applied to model the induction heating process in a Czochralski crystal growth system. The objective of this section is not to introduce a new theoretical framework, but to present the governing equations and assumptions relevant to the present numerical analysis.

The starting point for our discussion is Maxwell's equations and vector potential relation which is defined by:

$$\nabla \times \boldsymbol{A} = \boldsymbol{B} \qquad (1)$$

To reduce the computational complexity while preserving the essential physics of the induction heating process, the following assumptions are adopted:

1- The system is rotationally symmetric about the z-axis; therefore, all physical quantities are independent of the azimuthal coordinate φ.
2- All materials are assumed to be isotropic, non-magnetic, and electrically neutral.
3- The displacement current is neglected.
4- The electrical current and voltage distribution within the induction coil are assumed to be uniform.
5- The self-inductance of the RF induction coil is taken into account.
6- Both impressed and induced currents are assumed to operate under steady-state conditions; consequently, all electromagnetic field quantities vary harmonically with a single fixed frequency.

These assumptions are commonly employed in numerical studies of induction heating systems and are well justified for radio-frequency excitation and axisymmetric configurations. In particular, neglecting the displacement current is valid due to the relatively low operating frequencies compared to electromagnetic wave propagation scales, while the harmonic steady-state assumption allows the electromagnetic fields to be treated in the frequency domain. Under these assumptions, using Maxwell equations and vector potential definition, the governing equation can be written in MKS system as;

$$\frac{\partial}{\partial r}\left[\frac{1}{r}\frac{\partial}{\partial r}(rA_\varphi)+\frac{\partial^2 A_\varphi}{\partial z^2}\right]=-\mu J_\varphi \qquad (2)$$

Where A_φ is the azimuthal component of $\boldsymbol{A}$ and (r,φ,z) is the cylindrical coordinates. Equation (2) represents the governing differential equation for the azimuthal component of the magnetic vector potential in cylindrical coordinates. This formulation accounts for both the imposed current in the induction coil and the eddy currents induced in the conductive components of the system.

For numerical convenience and to simplify the solution of the governing equation, the magnetic vector potential formulation is recast in terms of the magnetic stream function, $\Psi_B = rA_\varphi$. This transformation enables an efficient treatment of the axisymmetric electromagnetic field and facilitates the finite element implementation.

$$\frac{\partial}{\partial r}\left(\frac{1}{r}\frac{\partial}{\partial r}(\Psi_B)\right)+\frac{\partial}{\partial z}\left(\frac{1}{r}\frac{\partial}{\partial z}(\Psi_B)\right)=-\mu J_\varphi$$

In which J_φ is defined as:

$$J_\varphi = J_d + J_e = J_d - \frac{\sigma}{r}\frac{\partial \Psi_B}{\partial t}$$

Where, σ is the electrical conductivity of each part, also J_d and J_e are the driving and eddy currents, respectively. Setting $J_d = J_0 \cos \omega t$ as the driving current in the coil, a solution can be expressed as:

$$\Psi_B(r,z,t) = C(r,z)cos\omega t + S(r,z)sin\omega t$$

Where, $C(r,z)$ is the in-phase component and $S(r,z)$ is the out-of-phase component of the solution. As a result, the electromagnetic problem reduces to a coupled set of elliptic partial differential equations for the real and imaginary components of the magnetic stream function, which are solved simultaneously to obtain the induced current distribution.

$$\frac{\partial}{\partial r}\left(\frac{1}{r}\frac{\partial S}{\partial r}\right)+\frac{\partial}{\partial z}\left(\frac{1}{r}\frac{\partial S}{\partial z}\right)=-\mu\frac{\sigma\omega}{r}C$$
$$\frac{\partial}{\partial r}\left(\frac{1}{r}\frac{\partial C}{\partial r}\right)+\frac{\partial}{\partial z}\left(\frac{1}{r}\frac{\partial C}{\partial z}\right)=-\mu(J_0-\frac{\sigma\omega}{r}S)$$

After solving (6) for $C(r,z)$ and $S(r,z)$, we can calculate the volumetric power generation in the metallic parts via:

$$q(r,z)=\frac{\omega}{2\pi}\int_0^{2\pi/\omega}P(r,z,t)\,dt=\frac{\sigma\omega^2}{2r^2}\left[C^2+\left(\frac{J_0 r}{\sigma\omega}-S\right)^2\right]$$

The volumetric power density obtained from Eq. (7) represents the local Joule heating generated by the induced eddy currents, which serves as the primary heat source in the subsequent thermal analysis.

In the above-mentioned equations, certain parameters, such as the electrical conductivity σ and the impressed current density J_0, take different values in different regions of the computational domain. The boundary conditions are specified as $\Psi_B = 0$ both in the far field $(r, z \to \infty)$ and along the axis of symmetry (r =

0) .These boundary conditions ensure the physical decay of the electromagnetic field in the far field and enforce symmetry along the central axis, which is consistent with the cylindrical geometry of the system. Due to the cylindrical symmetry of the considered setup, the problem can be treated as two-dimensional by eliminating the dependence on the azimuthal coordinate φ. Since induced heat is generated only within the metallic components of the system, the numerical calculations are restricted to these regions, as shown in Figure 2. The induction coil consists of eight hollow rectangular copper turns. Owing to the efficient water-cooling systems commonly employed in practical induction heating applications, the coil temperature is assumed to remain close to room temperature. As a result, temperature-dependent variations in the electrical conductivity of the induction coil are neglected.

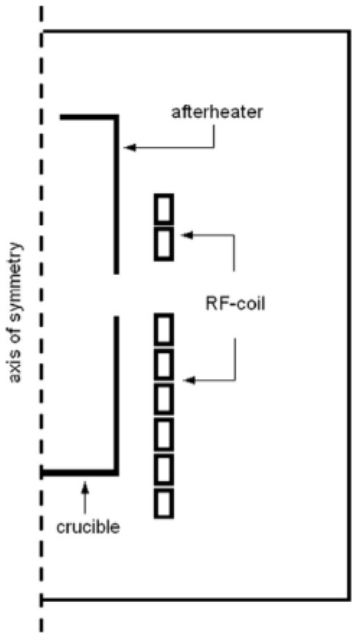

Figure 2: Metallic components of the axisymmetric Czochralski crystal growth system considered in the numerical model.

The magnetic permeability μ is assumed to be uniform throughout the computational domain and equal to the permeability of free space, i.e., $\mu = \mu_r \mu_0 = \mu_0$, where $\mu_r = 1$ denotes the relative magnetic permeability. The electrical conductivity of the crucible material (iridium) is taken as 1.72×10^6 $(\Omega.m)^{-1}$. To investigate the influence of the induction coil electrical conductivity, this parameter is varied over the range 5×10^4 $(\Omega.m)^{-1}$ to 1.5×10^8 $(\Omega.m)^{-1}$.

3. Results and Discussion

In Czochralski crystal growth systems, the spatial distribution and magnitude of heat generated within the crucible play a crucial role in determining thermal gradients, melt convection, and the stability of the solid–liquid interface. Therefore, the results are discussed with particular emphasis on how variations in induction coil electrical conductivity influence the heat distribution, total generated power, and overall heating efficiency.

Figure 3 illustrates the spatial distribution of the induced heat within the crucible for four different values of the induction coil electrical conductivity. As shown, the pattern of heat generation is strongly affected by variations in coil conductivity. At low conductivity values, the induced heat exhibits a highly non-uniform distribution characterized by steep thermal gradients along the crucible wall. In contrast, increasing the electrical conductivity of the induction coil leads to a noticeably smoother heat distribution, indicating a more uniform penetration of the induced eddy currents into the crucible.

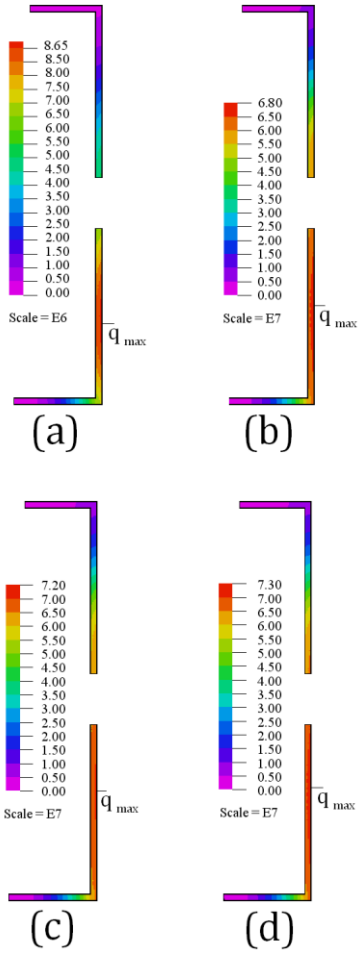

Figure 3: Spatial distribution of the induced heat within the crucible for four different values of induction coil electrical conductivity: (a) 5×10^4, (b) 1×10^6, (c) 1×10^7 and (d) 1.5×10^8 $(\Omega.m)^{-1}$.

A prominent feature observed in all cases is that the maximum heat generation occurs near the outer surface of the crucible wall. This behavior is primarily associated with the skin effect and the electromagnetic coupling between the induction coil and the conductive crucible. As the electrical conductivity of the induction coil increases, the location of this maximum heat generation gradually shifts upward along the crucible wall. This upward movement becomes less pronounced at higher conductivity values, suggesting that the electromagnetic coupling approaches a saturated regime beyond a certain conductivity threshold.

The observed reduction in thermal gradients with increasing coil conductivity can be attributed to the decrease in ohmic losses within the induction coil itself. Higher conductivity allows a larger fraction of the supplied electromagnetic power to be transferred to the crucible rather than being dissipated in the coil. Consequently, the induced current distribution within the crucible becomes more uniform, resulting in smoother volumetric Joule heating.

From the perspective of Czochralski crystal growth, such changes in heat distribution are of considerable importance. A more uniform thermal field within the crucible can contribute to reduced thermal stresses, improved stability of the melt flow, and a more controlled solid–liquid interface shape. Additionally, the axial shift of the maximum heat generation region may influence the vertical temperature gradient in the melt, which is a key parameter affecting crystal diameter control and growth stability. Therefore, the results presented in Figure 3 highlight the critical role of induction coil electrical conductivity in tailoring the thermal environment of Czochralski crystal growth systems.

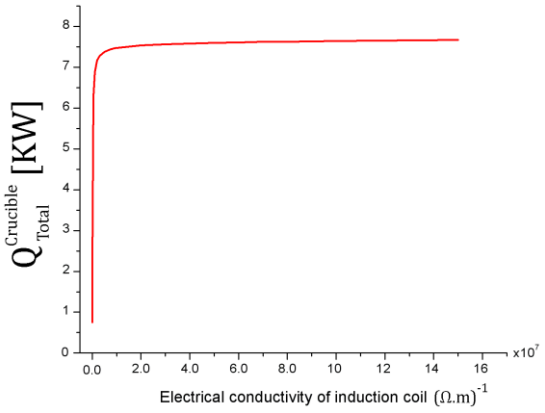

Figure 4: Variation of the total heat generated within the crucible as a function of induction coil electrical conductivity.

Figure 4 presents the variation of the total heat generated within the crucible as a function of the induction coil electrical conductivity. As shown, the amount of induced heat increases monotonically with increasing coil conductivity. However, the rate of this increase is not uniform over the entire conductivity range. At low conductivity values, a relatively small increase in coil conductivity results in a sharp rise in the generated heat, whereas at higher conductivities the growth rate becomes significantly more gradual. This behavior can be explained by considering the distribution of electromagnetic power losses within the system. At low electrical conductivities, a substantial portion of the supplied electromagnetic energy is dissipated as ohmic losses within the induction coil itself, leaving only a limited fraction available for heat generation in the crucible. As the coil conductivity increases, these internal losses are markedly reduced, allowing a larger share of the input power to be transferred to the crucible and converted into useful Joule heating.

Beyond a certain conductivity level, further increases lead to diminishing returns in terms of additional heat generation within the crucible. In this regime, the electromagnetic coupling between the coil and the crucible approaches an optimal condition, and the system performance becomes less sensitive to further improvements in coil conductivity. This saturation-like behavior indicates that extremely high conductivities may not yield proportionally higher heating efficiency.

From the perspective of Czochralski crystal growth, the results shown in Figure 4 highlight the importance of selecting an appropriate induction coil material. Sufficient heat generation within the crucible is essential to maintain the melt in a stable liquid state, while excessive energy losses can adversely affect process efficiency. Therefore, optimizing the electrical conductivity of the induction coil represents an effective strategy for achieving adequate heating power with reduced energy consumption in practical crystal growth systems.

Figure 5 illustrates the spatial distribution of the induced heat within the induction coil for four different values of electrical conductivity. At low conductivity values, the generated heat exhibits a highly non-uniform pattern characterized by strong local gradients and pronounced hot spots, particularly at the corners of the coil cross-section. This behavior is mainly attributed to proximity and edge effects, which intensify current crowding in regions with sharp geometric features.

As the electrical conductivity of the induction coil increases, the magnitude of these local thermal gradients decreases significantly, leading to a more uniform heat distribution along the coil turns. Although the maximum heat generation remains concentrated near the coil corners even at high conductivity values, the overall temperature non-uniformity is substantially

reduced. This indicates that higher conductivity materials effectively mitigate localized resistive losses within the coil.

From a practical standpoint, excessive and non-uniform heat generation in the induction coil is undesirable, as it increases cooling requirements and may adversely affect the mechanical integrity and operational lifetime of the coil. Therefore, the observed reduction in internal coil heating with increasing conductivity highlights the importance of material selection in the design of efficient and reliable induction heating systems.

Figure 6 shows the variation of the total heat generated within the induction coil as a function of its electrical conductivity. As evident from the figure, the total induced heat in the coil decreases rapidly with increasing conductivity in the low-conductivity regime. In this range, even modest improvements in conductivity lead to a substantial reduction in ohmic losses within the coil.

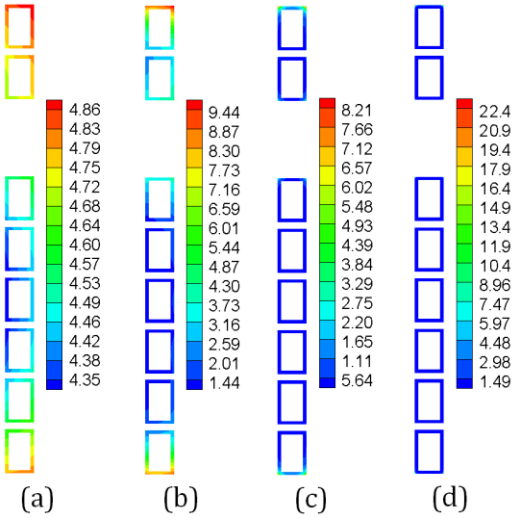

Figure 5: Spatial distribution of the induced heat within the induction coil for four different values of induction coil electrical conductivity: (a) 5×10^4, (b) 1×10^6, (c) 1×10^7 and (d) 1.5×10^8 $(\Omega.m)^{-1}$.

At higher conductivity values, the rate of decrease in generated heat becomes more gradual, indicating that the coil losses approach a minimum threshold determined by the electromagnetic field distribution and geometric constraints. This trend suggests that beyond a certain conductivity level, further enhancements yield diminishing returns in terms of loss reduction.

These results are particularly significant for practical induction heating systems, where minimizing coil losses is essential for improving energy efficiency and reducing the demand on cooling systems. The substantial reduction in heat generation within the coil at higher conductivities directly complements the increased heat generation observed in the crucible, as discussed in the previous section.

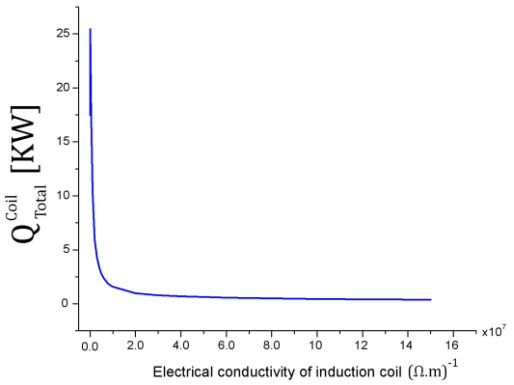

Figure 6: Variation of the total heat generated within the induction coil as a function of induction coil electrical conductivity.

Table 1 :Total generated heat in the crucible and induction coil, and the corresponding heating efficiency of the induction system for selected values of induction coil electrical conductivity.

Induction coil Conductivity $(\Omega.m)^{-1}$	$Q_{Total}^{Crucible}$ (kW)	Q_{Total}^{coil} (kW)	Efficiency (%)
5×10^4	0.7	17.4	4.1
1×10^6	6.8	10.400	40
1×10^7	7.4	1.5	83
1.5×10^8	7.6	0.3	95

Table 1 summarizes the calculated heating efficiency of the induction system for selected values of induction coil electrical conductivity. At low conductivity values, the efficiency is extremely low, indicating that the majority of the supplied electromagnetic power is dissipated within the induction coil rather than contributing to useful heat generation in the crucible. Such conditions are clearly unsuitable for practical crystal growth applications.

As the coil conductivity increases, a dramatic improvement in system efficiency is observed. The efficiency rises sharply from only a few percent at low conductivities to values exceeding 80% at higher conductivities. This significant enhancement reflects the effective redistribution of electromagnetic power from internal coil losses to useful Joule heating within the crucible.

At the highest conductivity considered, the system achieves an efficiency of approximately 95%, demonstrating that most of the supplied power is effectively utilized for heating the crucible. These results clearly indicate that induction coil electrical conductivity is a dominant factor governing the overall performance of induction-heated Czochralski crystal growth systems. Consequently, careful selection of high-conductivity coil materials can play a crucial role in improving energy efficiency, reducing operational costs, and enhancing the thermal stability of crystal growth processes.

4. Conclusion

In this study, the influence of induction coil electrical conductivity on heat generation and distribution within an induction-heated Czochralski crystal growth system was investigated numerically using a coupled electromagnetic model. The results demonstrate that the electrical conductivity of the induction coil plays a critical role in determining both the spatial characteristics of the thermal field and the overall heating efficiency of the system.

The numerical simulations reveal that at low coil conductivities, the induced heat within the crucible exhibits strong spatial non-uniformity, accompanied by steep thermal gradients. Concurrently, a significant portion of the supplied electromagnetic energy is dissipated within the induction coil itself. As the coil conductivity increases, the heat distribution in the crucible becomes progressively more uniform, and the total generated heat within the crucible increases substantially. In parallel, the heat generated within the induction coil decreases markedly, leading to a significant reduction in internal power losses.

Furthermore, the results indicate the existence of a conductivity threshold beyond which further increases in coil conductivity yield diminishing returns in heating performance. In this regime, the electromagnetic coupling between the induction coil and the crucible approaches an optimal condition, and the system efficiency attains values exceeding 90%. This behavior highlights the importance of selecting appropriate high-conductivity materials for induction coils in practical crystal growth applications. Overall, the findings of this work emphasize that careful optimization of induction coil electrical conductivity can significantly enhance heating efficiency, reduce energy losses, and improve the thermal environment within the crucible. These improvements are expected to contribute to enhanced thermal stability and more controlled growth conditions in Czochralski crystal growth processes. This numerical study provides valuable insights for the design and optimization of induction heating systems employed in crystal growth technologies.

Authors' Contributions

Hossein Karbaschi: Conceptualization, Methodology, Software, Data Curation, Visualization, Writing – Original Draft, Writing – Review & Editing. Mohammad Hossein Tavakoli: Supervision, Methodology, Validation, Formal Analysis.

Conflict of Interest

The authors declare no conflict of interest.

Acknowledgments

Hossein Karbaschi acknowledges the support provided by the Mahallat Institute of Higher Education.

References

1. Semiatin, S.L. Elements of Induction Heating: Design, Control, and Applications, ASM International, 1988. https://doi.org/10.31399/asm.tb.eihdca

2. Tavakoli, M.H.; et al. *Computational Modeling of Induction Heating Process*, Progress in Electromagnetics Research Letters, 2009. *11*, pp. 93-102. https://doi.org/10.2528/PIERL09071509

3. Tavakoli, M.H.; et al. *Computational Study of Electromagnetic Fields, Eddy Currents and Induction Heating in Thin and Thick Workpieces*, Communications in Computational Physics, 2010. *8 (1)*, pp. 211-225. https://doi.org/10.4208/cicp.2009.09.107

4. Rudnev, V.; et al. *Handbook of Induction Heating*, CRC Press, 2017. https://doi.org/10.1201/9781315117485

5. Tavakoli, M.; Karbaschi, H. *Numerical Study of Influences of the Input Current Frequency on the Induction Heating Process*, Progress in Physics of Applied Materials, 2021. *1 (1)*, pp. 44-49. https://doi.org/10.22075/ppam.2021.23704.1009

6. Shokri, A.J. *Numerical Study of Frequency Effect on Induction Heating Process in Three Dimensional*, Progress in Physics of Applied Materials, 2024. *4 (1)*, pp. 21-26. https://doi.org/10.22075/ppam.2024.32977.1083

7. Khazaal, M.H.; Abdulbaqi, I.M. *Modeling, Design and Analysis of an Induction Heating Coil for Brazing Process Using FEM*, AIC-MITCSA, IEEE, 2016. pp. 1-6. https://doi.org/10.1109/AIC-MITCSA.2016.7759918

8. Skeeba, V.Y.; et al. *Peculiarities of High-Energy Induction Heating During Surface Hardening in Hybrid Processing Conditions*, Metals, 2021. *11 (9)*, p. 1354. https://doi.org/10.3390/met11091354

9. Stević, Z.; et al. *The Design of a System for the Induction Hardening of Steels Using Simulation Parameters*, Applied Sciences, 2023. *13 (20)*, p. 11432. https://doi.org/10.3390/app132011432

10. Lu, L.; et al. *Numerical Study of Titanium Melting by High Frequency Inductive Heating*, International Journal of Heat and Mass Transfer, 2017. *108*, pp. 2021-2028. https://doi.org/10.1016/j.ijheatmasstransfer.2017.01.062

11. Dawson, F.P.; Jain, P. *A Comparison of Load Commutated Inverter Systems for Induction Heating*

and Melting Applications, IEEE Transactions on Power Electronics, 1991. *6 (3)*, pp. 430-441. https://doi.org/10.3390/en14206634
12. Tavakoli, M.H.; et al. *Influence of Coil Geometry on the Induction Heating Process in Crystal Growth Systems*, Journal of Crystal Growth, 2009. *311 (6)*, pp. 1594-1599. https://doi.org/10.1016/j.jcrysgro.2009.01.092
13. Tavakoli, M.H.; et al. *Numerical Study of Induction Heating in Melt Growth Systems—Frequency Selection*, Journal of Crystal Growth, 2010. *312 (21)*, pp. 3198-3203. https://doi.org/10.1016/j.jcrysgro.2010.07.035
14. Khodamoradi, H.; et al. *Influence of Crucible and Coil Geometry on the Induction Heating Process in Czochralski Crystal Growth System*, Journal of Crystal Growth, 2015. *421*, pp. 66-74. https://doi.org/10.1016/j.jcrysgro.2009.07.013
15. Friedrich, J.; et al. *Czochralski Growth of Silicon Crystals*, Handbook of Crystal Growth, Elsevier, 2015. pp. 45-104. https://doi.org/10.1016/B978-0-444-63303-3.00002-X
16. Hadidchi, S.; Tavakoli, M.H. *Influence of Temperature Dependence of Electrical Conductivity of Graphite Crucible in Czochralski Crystal Growth: A Numerical Analysis*, Progress in Physics of Applied Materials, 2023. *3 (2)*, pp. 131-139. https://doi.org/10.22075/ppam.2023.32556.1073
17. Wermiński, M.; et al. *Evaluation of Data Transfer Influence in Coupled Monte Carlo Finite Element Model on Microstructure Evolution Predictions*, Materials Research Proceedings, 2023. *28*. https://doi.org/10.1007/s00170-025-15323-2
18. Dezfoli, A.R.A. *Review of Simulation and Modeling Techniques for Silicon Czochralski Crystal Growth*, Journal of Crystal Growth, 2024. *648*, p. 127921. https://doi.org/10.1016/j.jcrysgro.2024.127921
19. Khodamoradi, H.; Tavakoli, M. *Thermal Analysis of Coil-Crucible Configurations in Czochralski Growth of BGO Crystals*, Progress in Physics of Applied Materials, 2026. *6 (2)*, pp. 127-135. https://doi.org/10.22075/ppam.2025.38367.1157